



ELSEVIER

Journal of Alloys and Compounds 330–332 (2002) 472–475

Journal of
ALLOYS
AND COMPOUNDS

www.elsevier.com/locate/jallcom

The effect of N_2^+ and C^+ implantation on uranium hydride nucleation and growth kinetics

R. Arkush^a, M. Brill^a, S. Zalkind^a, M.H. Mintz^{a,b}, N. Shamir^{a,*}^aNuclear Research Center – Negev, P.O. Box 9001, 84190 Beer-Sheva, Israel^bBen-Gurion University of the Negev, P.O. Box 653, Beer-Sheva, Israel

Abstract

Hydrogen attack on uranium and uranium alloys may cause embrittlement and hydride formation that are undesirable in nuclear fuel technology. Implantation of the uranium surface by a high dose of energetic ions modifies the surface in a way that delays the hydrogen attack and slows the growth rate of the hydride. The implanted surfaces also exhibited better passivation to air oxidation. In the present study, 45 keV N_2^+ and C^+ ions with a dose of $6 \cdot 10^{17}$ ions/cm² were implanted (separately) in pure uranium. The incipient hydriding nucleation and growth kinetics of the implanted uranium samples were measured in a hot-stage microscopy system. The surface was continuously monitored, during the hydrogenation process, by a TV camera and recorded on videotape. The reaction was stopped, for various experiments, at different reaction steps by pumping the hydrogen out. SEM micrographs revealed, especially for the C^+ implanted samples, a morphology in which the hydride appears as blisters, seemingly under the implanted layer. The hot-stage micrographs were analyzed by image-analysis procedures yielding the nucleation and growth rates for the implanted vs. unimplanted specimens. Possible explanations are suggested for the passivation effects imparted by ion implantation. © 2002 Elsevier Science B.V. All rights reserved.

Keywords: Ion implantation; Growth kinetics; Nucleation; Uranium hydride; Passivation

1. Introduction

Hydrogen attack on uranium and uranium alloys may cause embrittlement and hydride formation, which are undesirable in nuclear fuel technology. Uranium and uranium alloys react easily with hydrogen to form uranium hydride (for recent reviews see Ref. [1]). The hydriding reaction of massive uranium samples has been reported to start on the surface with (visually observed) hydride nuclei, growing on the surface, overlapping and finally forming a continuous layer [1–7]. The kinetics of the hydrogen–uranium reaction has been extensively studied. Hot-stage microscopy (HSM, see next section) experiments yielded the dependence of nuclei density and growth kinetics on temperature, pressure [5–7], sample microstructure [8], specifics of the oxide layer and the effect of defects and inclusions [9]. In the early HSM experiments [3,4] as well as those reported in the present study, more than one type (or family) of hydride nuclei was observed.

Ion implantation is a well-known method for protection

of metals against wear, fatigue and corrosion [10]. Other studies deal with ion implantation of uranium and U–0.2 wt.% V, for prevention of the hydriding reaction: O_2^- [11], C^+ [12], N_2^+ , Si^+ and S^+ [13], implanted in various doses and energies, all reduce and slow the hydriding of the metal substrate.

2. Experimental

2.1. Implanted layer formation and characterization

The samples, implantation process and characterization of the implanted layers are fully described in a previous publication [14]. In short, 45 keV N_2^+ and C^+ ions with a dose of $6 \cdot 10^{17}$ ions/cm² were implanted (separately) in pure uranium and U–0.1 wt.% Cr. Depth profile Auger electron emission spectroscopy (AES) and X-ray diffraction (XRD) were used to characterize the implanted layer.

The implanted layer depth is about 60 nm for both implantations. For the N_2^+ implanted samples, the layer consists of U_2N_3 and UN_2 on the surface (oxidized to a depth of about 1–2 nm) with the nitrogen concentration

*Corresponding author. Tel.: +972-8-656-8785; fax: +972-8-656-8751.

E-mail address: nshamir@hotmail.com (N. Shamir).

decreasing gradually into the uranium bulk. The carbon concentration profile and the oxidation extent are similar for the C^+ implanted samples, where the surface consists of UC_2 .

2.2. Hydrogenation experiments and monitoring

The incipient hydriding nucleation and growth kinetics of the implanted uranium samples were measured in a HSM system [15]. The surface was continuously monitored, during the hydrogenation process, by a TV camera and recorded on videotape.

The specimens were first pretreated by heating to 200°C in a vacuum of $\sim 1 \cdot 10^{-5}$ Torr for 120 min, then exposed to ultra pure hydrogen under isobaric (1000 mbar) and isothermal (100°C) conditions (1 Torr = 133.322 Pa).

The micrographs in Fig. 1 show a typical sequence of surface hydriding process of an N_2^+ implanted U sample. The border between the implanted area (top right) and the unimplanted one (bottom left) is clearly seen. It can be clearly observed that hydrogen attack (black spots) occur almost only on the unimplanted area. The reaction was stopped, for various experiments, in different reaction steps by pumping the hydrogen out. XRD and scanning electron microscopy (SEM) were performed on the partially hydrogenated samples.

The XRD (not presented) yields strong UH_3 lines for the unimplanted side of the sample as compared to weak lines for the implanted side, in accordance with the HSM

micrographs. A set of SEM micrographs of a partially hydrogenated C^+ implanted U sample is presented in Fig. 2. It can be seen that the hydride morphology is that of blisters, seemingly under the implanted layer.

3. Analysis and discussion

The hot-stage micrographs were analyzed by image-analysis processes to evaluate nucleation and growth rates for the implanted vs. unimplanted specimens. The image analysis indicates an isotropic growth of the nuclei. Mean growth velocities and the time dependence of the nucleation rates were obtained. Fig. 3 presents the room temperature rate of hydride nucleation on the monitored area for the unimplanted and on the N_2^+ and C^+ implanted samples. Fig. 4 presents the time dependence of the percentage of the total surface area attacked by hydrogen (i.e. the convolution of both, nucleation and growth).

The SEM micrographs (Fig. 2) show that the hydride spreads beneath the implanted layer (in the non-implanted uranium this phenomenon is not observed). The spot where the hydride breaks through the implanted layer is clearly observed. The morphology (about the center of the isotropic blister) suggests that this is probably the initial nucleation site. At least for the nucleation spot observed in Fig. 2b and c (and for many others not shown here) it seems that nucleation occurs on an existing surface defect (one located on a scratch in this case). This makes sense

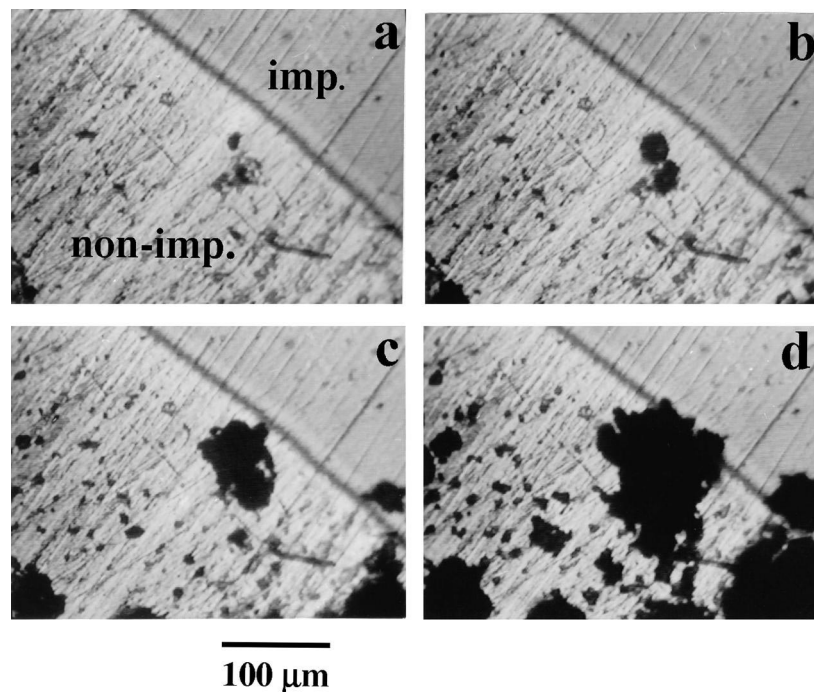


Fig. 1. A sequence ($\Delta t = 120$ s between frames) of hot-stage microscopy optical micrographs of uranium exposed to hydrogen ($P = 1000$ mbar; $T = 100^\circ\text{C}$). The difference in hydrogen attack is apparent between the N_2^+ implanted [indicated as 'imp.' in (a)] and non-implanted ['non-imp' in (a)] areas. The induction time corresponding to the commencement of the reaction is 302 s after exposure to hydrogen.

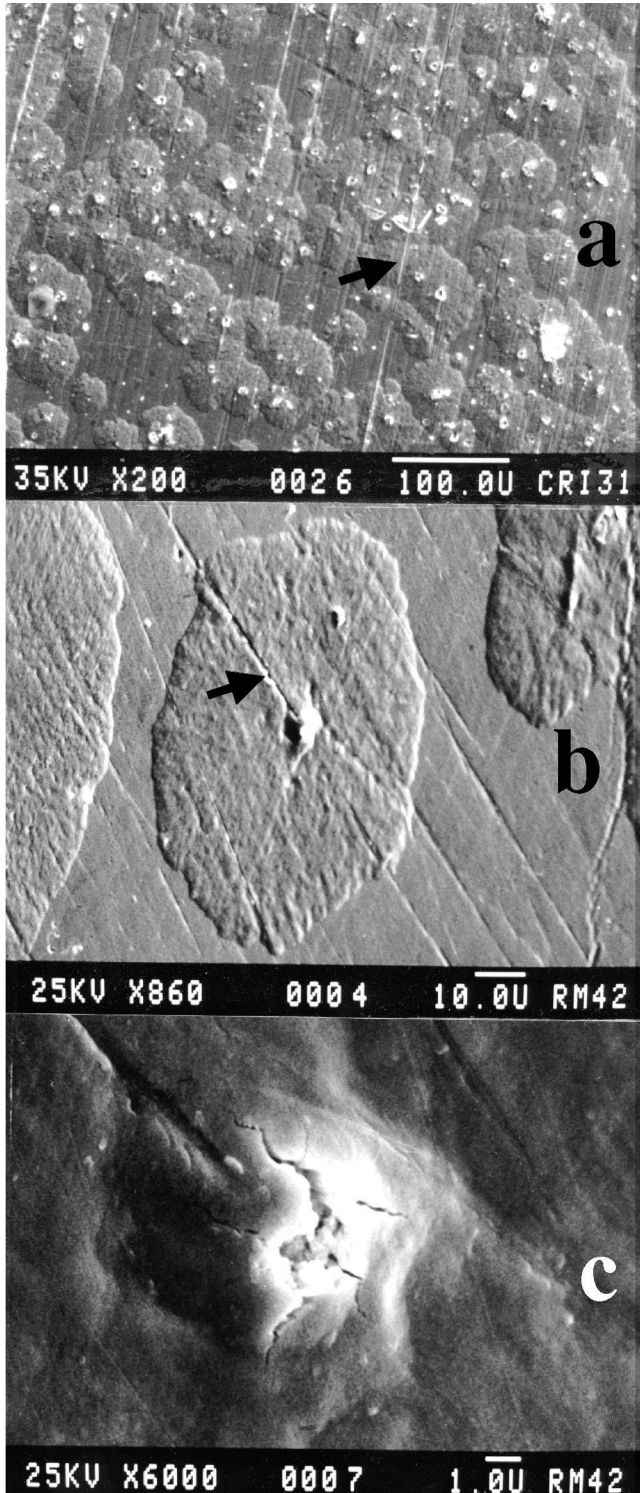


Fig. 2. SEM micrographs of hydrogen attack on a C^+ implanted uranium sample. (a) Blistered area; (b) specifics of a blister – the spot of oxide fracture and also supposedly the defect of nucleus origin (sitting on a scratch) is observed; (c) detailed micrograph of the defect presented in (b) – the cracking of the oxide can be seen. The arrows in (a) and (b) point at polishing scratches that run continuously from the non-attacked area to the top of the blister manifesting the fact that the blister grows under the implanted area.

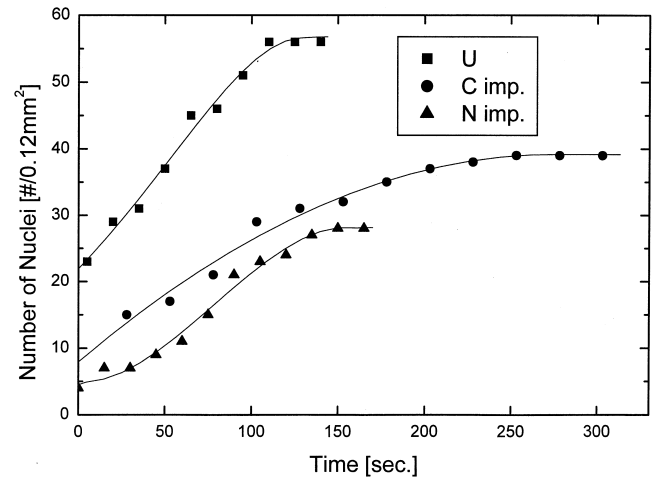


Fig. 3. Nucleation rate of hydride formation ($P=1000$ mbar; $T=100^\circ\text{C}$) vs. exposure time for the surfaces of pure, N_2^+ and C^+ implanted uranium.

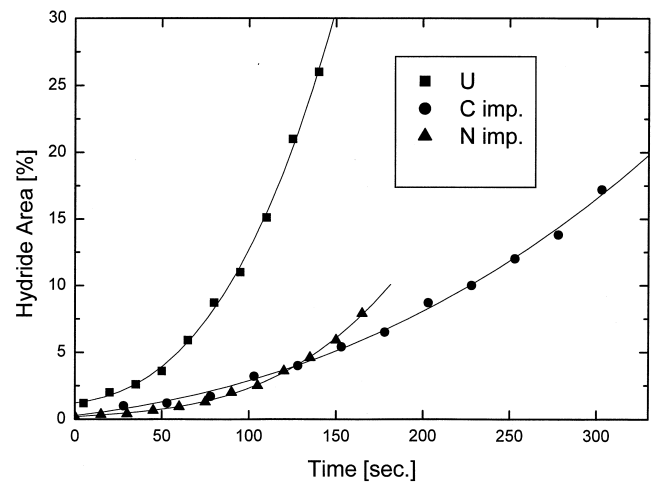


Fig. 4. Relative area of hydride formed vs. time for the samples and conditions of Fig. 3.

since such a defect is on the one hand an easier inlet route for hydrogen and on the other hand a relatively weak spot at which the implanted layer (on top of the hydride) is most likely to break as a result of the pressure applied by the swelling of the hydride.

The rate of nucleation (Fig. 3) displays the usual S shape behavior [5–7] of initial acceleration and final deceleration kinetics. The absolute number of nuclei as well as the nucleation rate and the final saturation number of nuclei is significantly higher for the unimplanted uranium sample than for both the carbon and nitrogen implanted ones (as can be seen in the hydrogenation micrographs – Fig. 1), where the latter seems to provide a slightly better protection for hydrogen attack.

The unit cell of the native oxide is more than 30% larger than that of uranium metal. This fact causes, as clearly presented in Ref. [14], fracture and cracking of the oxide, thus providing many inlet routes for hydrogen nucleation.

Also, a fractured oxide is lifted and removed easily by the hydride spreading beneath it, causing a large area of surface hydride through which hydrogen flows in at a high rate, enabling a fast growth of the hydride nuclei. On the other hand, the implanted layer, having a diffuse interface with the metal, with a gradual concentration gradient does not crack and forms a continuous adherent layer [14]. This induces a significantly smaller number of nucleation sites, probably at pre-existing defects, as observed in Fig. 2, and also makes it harder for the hydride to rapture the implanted layer. The spreading of the hydride in blisters beneath the implanted layer is slower than that of an exposed hydride. Only at some defect points the hydride succeeds to break the implanted layer and spreads similarly to the non-implanted surface hydride nuclei. This explains the lower number of hydride nuclei as well as their initial slower growth rate on the implanted surface as compared to the non-implanted ones.

4. Conclusion

Implantation of uranium by C^+ and N_2^+ ions forms a layer of carbide or nitride, which significantly reduces the hydride nucleation rate as well as the initial rate of growth of hydride nuclei. The carbide or nitride layers being adherent and rapture-resistant prevent the formation of the natural oxide, which is easily fractured due to its large mismatch with the metal. Cracks in the oxide are the major pathway of hydrogen into the metal, as well as ‘weak’ spots easily fractured by the expanding developing hydrides. Hence, the implanted layers provide a better protection against hydrogen attack.

References

- [1] J. Bloch, M.H. Mintz, The hydriding reaction of uranium, in: B. Mishra, W.A. Avriil (Eds.), *Actinide Processing Methods and Materials*, TMS, 1994, pp. 121–131;
- W. Bartscher, Actinides – hydrogen, in: F.A. Lewis, A. Aladjem (Eds.), *Hydrogen Metal Systems I*, Scitec, 1996, pp. 159–238, Chapter 5.
- [2] M.H. Mintz, J. Bloch, *Prog. Solid State Chem.* 16 (1985) 163.
- [3] L.W. Owen, R.A. Scudamore, *Corrosion Sci.* 6 (1966) 461.
- [4] J. Bloch, F. Simca, M. Kroupp, A. Stern, D. Shmariahu, M.H. Mintz, Z. Hadari, *J. Less-Common Met.* 103 (1984) 163.
- [5] J. Bloch, M.H. Mintz, *J. Less-Common Met.* 81 (1981) 301, and references cited therein.
- [6] M. Brill, J. Bloch, M.H. Mintz, *J. Alloys Comp.* 266 (1998) 180.
- [7] Y. Ben-Eliyahu, M. Brill, M.H. Mintz, *J. Chem. Phys.* 111 (1999) 6053.
- [8] D. Moreno, R. Arkush, S. Zalkind, N. Shamir, *J. Nucl. Mater.* 239 (1996) 181;
- M. Balooch, A.V. Hamza, *J. Nucl. Mater.* 230 (1996) 259.
- [9] R. Arkush, A. Venkert, M. Aizenshtein, S. Zalkind, D. Moreno, M. Brill, M.H. Mintz, N. Shamir, *J. Alloys Comp.* 244 (1996) 197.
- [10] I.J.R. Baumvol, in: J.F. Ziegler (Ed.), *Ion Implantation Science and Technology*, Academic Press, Orlando, FL, 1984, p. 261.
- [11] R.G. Musket, G. Robinson-Weis, R.G. Patterson, UCRL-89360 (1983).
- [12] R.G. Musket, UCRL-95609 (1987).
- [13] A. Ayrat, D. Crusset, G. Raboisson, *Mater. Res. Soc. Symp. Proc.* 268 (1992) 9;
- D. Crusset, Ph.D. Thesis (in French), Universite de Bourgogne, Dijon, 1992.
- [14] R. Arkush, M.H. Mintz, N. Shamir, *J. Nucl. Mater.* 281 (2000) 182.
- [15] R. Miche, F. Gabler, W. Wurtz, *Aluminium* 37 (1961) 652.